Nonlinear dynamics of an optomechanical system with a coherent mechanical pump: Second-order sideband generation

Hiroyuki Suzuki* and Eric Brown
School of Mathematics and Physics, University of Queensland, Brisbane QLD 4072, Australia

Ray Sterling†
Department of Mathematics, Royal Holloway, University of London, Egham, TW20 0EX Surrey, United Kingdom
(Received 20 May 2015; published 14 September 2015)

Second-order sideband generation in a coherent-mechanical pumped optomechanical system is discussed, and the features of the coherent mechanical pump induced enhancement of second-order sideband generation are identified. We show that the coherent mechanical pump induced enhancement of second-order sideband generation exhibits an essential difference between the case of a weak control field and a strong control field. In the weak control field case, the efficiency of second-order sideband generation increases as the amplitude of the mechanical pump increases. In the strong control field case, the effect of optomechanically induced transparency occurs and increasing the amplitude of the mechanical pump does not always bring an enhancement of second-order sideband generation. The phase-dependent effect of the second-order sideband generation with a coherent mechanical pump is also discussed, and it is shown that the phase difference ϕ plays an important role in the process of second-order sideband generation.

DOI: 10.1103/PhysRevA.92.033823 PACS number(s): 42.50.Wk, 03.65.Ta

I. INTRODUCTION

A generic optomechanical system consists of an optical Fabry-Perot cavity, in which one mirror is fixed while the another is movable and treated as a mechanical resonator with the effective mass m and frequency ω_m. Many novel effects arise due to the backaction of mechanical motion acting on the dynamics of the cavity field. Cavity optomechanics, which explores the coupling between the optical field and mechanical oscillation, has attracted great interest in the past ten years [1] due to its importance in both fundamental physics and practical applications, such as high-precision measurements and the manipulation of a mechanical vibrator on the quantum level [2].

Recently, nonlinear optomechanical interactions have emerged as an important new frontier in cavity optomechanics [3]. In the classical mechanism, nonlinear optomechanical interaction leads to sideband generation [4] and optomechanical chaos [5]. On the quantum level, nonlinear optomechanical interactions are predicted to exhibit large optical Kerr nonlinearity and photon blockade in the single-photon strong-coupling regime [6]. It has been shown that the preparation of nonclassical states in the internal dynamics can only be achieved in the nonlinear optomechanical interaction regime [1–3].

On the other hand, the introduction of the mechanical coherence by an additional coherent driving force has led to more complex quantum coherent and interference phenomena, and it is found that effects based on the linearized optomechanical interaction, such as optomechanically induced transparency and amplification, can be controlled by simply adjusting the phase and amplitude of the mechanical pump [7]. Further work shows that a large group delay of the output probe field can be achieved in the presence of the coherent mechanical pump [8].

Studying the nonlinear optomechanical interactions in the presence of a coherent mechanical pump is an interesting topic. It has been shown that there are second- and higher-order sideband generation in an optomechanical system due to the nonlinear optomechanical interactions [4]. The second-order sideband generation is that if the strong control field with frequency ω_1 and the weak probe field with frequency ω_p are incident upon the optomechanical system, then there are output fields with frequencies $\omega_1 \pm 2\Omega$ generation, where the frequency component $\omega_1 + 2\Omega$ is the second-order upper sideband while $\omega_1 - 2\Omega$ is the second-order lower sideband. The signals at the second-order sideband are of great importance in understanding the nonlinear optomechanical interactions, for example, the nonlinear quantum nature of the optomechanical interactions as well as the effect of photon blockade may be revealed even in the weak-coupling regime through the signal of optomechanically induced transparency at the second sideband [9–12]. Here we focus on the process of second-order sideband generation in the presence of a coherent mechanical driving force, and show that second-order sideband generation can be tuned by adjusting the phase and amplitude of the mechanical pump. Our discussions may also be applicable to a DNA–quantum-dot hybrid system [13] with a mechanical pump.

Experimentally, there are some ways to realize the coherent mechanical driving in the optomechanical system, such as using Josephson phase qubits [14], microwave electrical driven [15], and other time-varying weak forces. It's worth noting that a cascaded optical transparency was recently observed [16] by applying a mechanical driving to an optomechanical system with both the optomechanical coupling and parametric phonon-phonon coupling.

There are several advantages of the mechanical pump in optomechanical systems. First, increasing the power of the control field may reduce the controllability of the optomechanical systems. For example, when the power exceeds the 20 mW level, stimulated Raman scattering would inevitably appear [17], which may make the system too complicated for controlling the second-order sideband generation. Second,

*hiroyuksuzuki@gmail.com
†r.m.sterling@outlook.com

similar to the phaseonium systems, in which atomic coherences are generated by the direct drive at the microwave frequency [18], the mechanical pump can directly produce mechanical coherence in the optomechanical systems, which is useful in optomechanical control.

This paper is organized as follows. We give a derivation of second-order sideband generation under a coherent mechanical pump in Sec. II, where the amplitude of both the first- and second-order sideband are obtained analytically. In Sec. III, we discuss the features of coherent mechanical driving induced enhancement of second-order sideband generation, including the weak control field case and the strong control field case. In Sec. IV, the features of the phase-dependent effect are discussed. Finally, a conclusion of the results is summarized in Sec. V.

II. DERIVATION OF SECOND-ORDER SIDEBAND GENERATION IN THE PRESENCE OF A MECHANICAL PUMP

We consider that the optical cavity is driven by a strong control field and a relatively weak probe field. The frequency of the control field ω_1 is detuned by $\bar{\Delta}$ which approximately equals to $-\Omega_m$ from the cavity resonance frequency, and the frequency of the probe field ω_p is offset by the tunable frequency Ω from ω_1. The line width of the cavity resonance frequency is κ. An external coherent mechanical pump with amplitude s_m, frequency $\Omega = \omega_p - \omega_1$, and phase ϕ_m is imposed to the mechanical resonator. The Hamiltonian formulation [19] of such a system is

$$\hat{H} = \hat{H}_0 + \hat{H}_m + \hbar G\hat{x}\hat{a}^\dagger\hat{a} + i\hbar\sqrt{\eta\kappa}(\hat{a}^\dagger S_{\rm in} - \hat{a}S_{\rm in}^*), \quad (1)$$

with

$$\hat{H}_0 = \frac{\hat{p}^2}{2m} + \frac{m\omega_m^2\hat{x}^2}{2} + \hbar\omega_c\hat{a}^\dagger\hat{a}, \quad \hat{H}_m = -s_m\hat{x}\cos(\Omega t + \phi_m),$$
$$S_{\rm in} = s_1 e^{-i\omega_1 t} + s_p e^{-i(\omega_p t + \phi_p)}, \quad (2)$$

where $\hat{x}$ and $\hat{p}$ are the position and momentum operators of the mechanical resonator, respectively, $\hat{a}$ is the photon annihilation operator of the cavity fields, ω_c is the cavity resonance frequency, and G is the optomechanical coupling constant. κ is the total loss rate of the cavity fields and consists of an intrinsic loss rate κ_0 and the wave guide coupling rate $\kappa_{\rm ex}$. The coupling parameter $\eta = \kappa_{\rm ex}/\kappa$ can be continuously adjusted, and we choose $\eta = 1/2$ throughout the work [19]. $s_1 = \sqrt{P_1/\hbar\omega_1}$ and $s_p = \sqrt{P_p/\hbar\omega_p}$ with P_1 and P_p the powers of the control and probe field, respectively. ϕ_p is the phase difference between the probe and control fields.

In a frame rotating at ω_1, and introducing the decay rate γ_m of the mechanical oscillator phenomenologically, the Heisenberg-Langevin equations, which describe the evolutionary dynamics of the optomechanical system, can be obtained as follows:

$$\begin{aligned}\dot{\hat{a}} &= -[\kappa/2 + i(-\Delta + G\hat{x})]\hat{a} + \sqrt{\eta\kappa}[s_1 + s_p e^{-i(\Omega t+\phi_p)}] \\ &\quad + \sqrt{\eta'\kappa}\hat{a}_{\rm in}, \\ \dot{\hat{x}} &= \hat{p}/m, \\ \dot{\hat{p}} &= -m\omega_m^2\hat{x} - \hbar G\hat{a}^\dagger\hat{a} - \gamma_m\hat{p} + s_m\cos(\Omega t + \phi_m) + \hat{F}_{\rm th},\end{aligned} \quad (3)$$

where $\Delta = \omega_1 - \omega_c$, $\eta' = 1 - \eta$, and $\hat{a}_{\rm in}$ and $\hat{F}_{\rm th}$ are the quantum and thermal noises of the mechanical oscillator and the cavity, respectively, with $\langle\hat{a}_{\rm in}(t)\hat{a}_{\rm in}^\dagger(t')\rangle = \delta(t-t')$, $\langle\hat{a}_{\rm in}(t)\rangle = 0$, $\langle\hat{F}_{\rm th}(t)\hat{F}_{\rm th}^\dagger(t')\rangle = \gamma_m\int e^{-i\omega(t-t')}[\coth(\hbar\omega/2k_BT)+1]d\omega/2\pi\omega_m$, and $\langle\hat{F}_{\rm th}(t)\rangle = 0$.

In the present work, we focus on the mean response of this system, so we can reduce the operators to their expectation values, viz., $\langle\hat{x}\rangle = x$, $\langle\hat{p}\rangle = p$, $\langle\hat{a}\rangle = a$, and the noise terms can be dropped because of the properties $\langle\hat{a}_{\rm in}(t)\rangle = 0$ and $\langle\hat{F}_{\rm th}(t)\rangle = 0$. The reduced Heisenberg equations then become

$$\ddot{x} + \gamma_m\dot{x} + \omega_m^2 x = -\alpha|a|^2 + \beta\cos(\Omega t + \phi_m), \quad (4)$$

$$\dot{a} = -[\kappa/2 + i(-\Delta + Gx)]a + \sqrt{\eta\kappa}[s_1 + s_p e^{-i(\Omega t+\phi_p)}], \quad (5)$$

where $\alpha = \hbar G/m$ and $\beta = s_m/m$. Equations (4) and (5) are nonlinear and coupled equations due to the parametric coupling between the optical and mechanical modes. The linearization of Eqs. (4) and (5), which corresponds to the linearized dynamics of the optomechanical system with a mechanical driving, are studied in Refs. [7,8], where optomechanically induced transparency and slow light have been discussed. To discuss second-order sideband generation, the nonlinearity of these equations must be taken account. We can calculate the amplitudes of the first- and second-order sideband by using the following ansatz [4]:

$$\begin{aligned}x &= x_0 + X_1 e^{-i\Omega t} + X_1^* e^{i\Omega t} + X_2 e^{-2i\Omega t} + X_2^* e^{2i\Omega t}, \\ a &= a_0 + A_1^- e^{-i\Omega t} + A_1^+ e^{i\Omega t} + A_2^- e^{-2i\Omega t} + A_2^+ e^{2i\Omega t},\end{aligned} \quad (6)$$

Substituting Eqs. (6) into Eqs. (4) and (5) leads to six algebra equations: three of them describe the process of the first-order sideband which corresponds to the linear case, while the other three equations describe the amplitude of the second-order sideband generation. After some derivation, we can obtain A_1^-, and A_2^- as follows:

$$A_1^- = \Phi_p(\Omega)\sqrt{\eta\kappa}s_p e^{-i\phi_p} - iGa_0 s_m e^{-i\phi_m}\Phi_m(\Omega)/2, \quad (7)$$

$$A_2^- = e^{-i\phi'}\left[s_m\theta_1(\Omega) + s_m\theta_2(\Omega) + s_m^2 C_4(\Omega)e^{-i\phi} + C_5(\Omega)e^{i\phi}\right], \quad (8)$$

with

$$\begin{aligned}\Phi_p(\Omega) &= [1 + i\cdot f(\Omega)]/\varepsilon(\Omega), \qquad \Phi_m(\Omega) = \chi(\Omega)/\varepsilon(\Omega), \\ \varepsilon(\Omega) &= 2\bar{\Delta}f(\Omega) + \kappa/2 - i(\bar{\Delta} + \Omega), \\ f(\Omega) &= \hbar a_0\chi(\Omega)D_1(\Omega), \qquad \chi(\Omega) = 1/\delta(\Omega), \\ \delta(\Omega) &= m\left(\omega_m^2 - \Omega^2 - i\gamma_m\Omega\right), \\ \theta_1(\Omega) &= C_1(\Omega)C_3(\Omega)D_4(\Omega) + 2C_2(\Omega)D_3(\Omega)D_4(\Omega), \\ \theta_2(\Omega) &= \sqrt{\eta\kappa}s_p\Phi_p(\Omega)C_1(\Omega)D_3(\Omega), \\ \sigma_1(\Omega) &= i\alpha G/(-2i\Omega + \tau^*), \\ \sigma_2(\Omega) &= i\alpha G/(-2i\Omega + \tau), \\ B(\Omega) &= \delta(2\Omega) + \sigma_1(\Omega)|a_0|^2, \\ C_1(\Omega) &= [iGB(\Omega) + \alpha D_1(\Omega)]/D_2(\Omega), \\ C_2(\Omega) &= \sigma_1(\Omega)D_1(\Omega)/D_2(\Omega), \\ C_3(\Omega) &= -iG\Phi_m(\Omega)a_0/2,\end{aligned}$$

$$C_4(\Omega) = C_1(\Omega)C_3(\Omega)D_3(\Omega) + C_2(\Omega)[D_3(\Omega)]^2,$$
$$C_5(\Omega) = \sqrt{\eta\kappa}s_p C_1(\Omega)\Phi_p(\Omega)D_4(\Omega) + C_2(\Omega)[D_4(\Omega)]^2,$$
$$D_1(\Omega) = G^2 a_0^*/(-i\Omega + \tau^*),$$
$$D_2(\Omega) = (2i\Omega - \tau)[B(\Omega) - \sigma_2(\Omega)|a_0|^2],$$
$$D_3(\Omega) = \Phi_m(\Omega)(\tau - i\Omega)/2,$$
$$D_4(\Omega) = \sqrt{\eta\kappa}s_p[(\Omega + i\tau)\Phi_p(\Omega) - 1]/Ga_0, \quad (9)$$

where $\phi = \phi_m - \phi_p$, $\phi' = \phi_m + \phi_p$, $x_0 = -\hbar G|a_0|^2/m\omega_m^2$, $a_0 = \sqrt{\eta\kappa}s_1/\tau$, $\tau = \kappa/2 - i\bar{\Delta}$, and $\bar{\Delta} = \Delta - Gx_0$. The amplitude at the frequency of the probe field consists of two terms in Eq. (7): the first term presents the driving source from the probe field, while the other term arises from the mechanical pump. The phase difference between two sources, $\phi_p - \phi_m$, plays an important role in the phenomena of optomechanically induced transparency and slow light. For the case that $s_m = 0$, viz., there is no mechanical pump, Eqs. (7) and (8) reduce to $A_1^- = \Phi_p(\Omega)\sqrt{\eta\kappa}s_p e^{-i\phi_p}$ and $A_2^- = C_5(\Omega)e^{-2i\phi_p}$, which is exactly the results obtained in previous works [4,19].

The output field of the optomechanical system can be obtained by using the input-output relation $S_{\rm out} = S_{\rm in} - \sqrt{\eta\kappa}a$. In a frame rotating at ω_1, the output fields are

$$S_{\rm out} = c_0 + c_1^- e^{-i\Omega t} + c_1^+ e^{i\Omega t} + c_2^- e^{-2i\Omega t} + c_2^+ e^{2i\Omega t}, \quad (10)$$

where $c_0 = s_1 - a_0\sqrt{\eta\kappa}$, $c_1^- = s_p e^{-i\phi_p} - \sqrt{\eta\kappa}A_1^-$, $c_1^+ = -\sqrt{\eta\kappa}A_1^+$, $c_2^- = -\sqrt{\eta\kappa}A_2^-$, and $c_2^+ = -\sqrt{\eta\kappa}A_2^+$. The transmission of the probe field is defined as $t_p = c_1^-/s_p e^{-i\phi_p}$, and can be obtained as follows:

$$t_p = 1 - \eta\kappa\Phi_p(\Omega) - \sqrt{\eta\kappa}\frac{s_m}{s_p}C_3(\Omega)e^{-i\phi}. \quad (11)$$

If there is no mechanical pump, viz. $s_m = 0$, then

$$t_p = 1 - \eta\kappa\Phi_p(\Omega) = 1 - \eta\kappa\frac{1 + i\cdot f(\Omega)}{\kappa/2 - i(\bar{\Delta} + \Omega) + 2\bar{\Delta}f(\Omega)}, \quad (12)$$

which has been obtained and discussed in detail in previous works [19]. The mechanical pump results in a phase-dependent modification of the transmission, which has been discussed by Jia *et al.* [7].

The term of $c_2^- e^{-2i\Omega t}$ describes the second-order upper sideband process, in which the output field with the frequency $\omega_1 + 2\Omega$ can be produced, while the term of $c_2^+ e^{2i\Omega t}$ describes the second-order lower sideband process, in which the output field with the frequency $\omega_1 - 2\Omega$ can be produced. In what follows, we will give a discussion on the amplitude of the second-order upper sideband. One also can discuss the amplitude of the second-order lower sideband similarly.

III. COHERENT MECHANICAL PUMP INDUCED ENHANCEMENT OF SECOND-ORDER SIDEBAND GENERATION

To describe the process of second-order sideband generation, we use the efficiency of second-order sideband generation [4] $\eta_s = |-\sqrt{\eta\kappa}A_2^-/s_p e^{-i\phi_p}|$, which can be obtained as follows:

$$\eta_s = \sqrt{\eta\kappa}|M_1(\Omega) + s_{mp}s_m C_4(\Omega)e^{-i\phi} + \eta\kappa s_p M_2(\Omega)e^{i\phi}|, \quad (13)$$

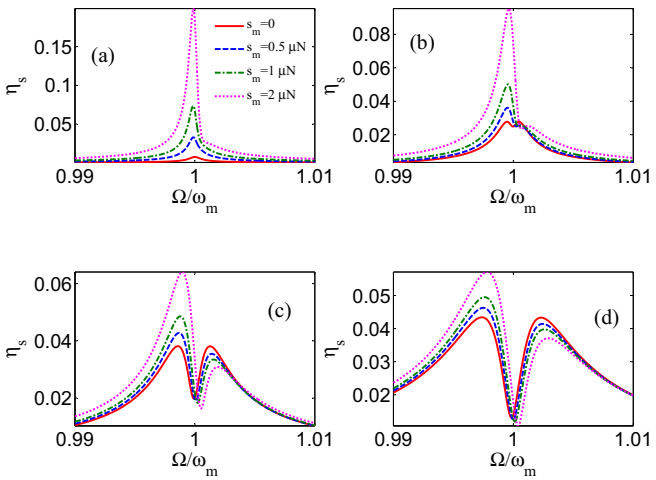

FIG. 1. (Color online) The efficiency of second-order sideband generation η_s as a function of Ω under different mechanical pumps and control fields. The powers of the control field are (a) 10, (b) 100, (c) 300, and (d) 600 μW. The other parameters are $\Omega_m/2\pi = 51.8$ MHz, $m = 20$ ng, $G/2\pi = -12$ GHz/nm, $\Gamma_m/2\pi = 41.0$ kHz, $\kappa/2\pi = 15.0$ MHz, $\Delta = -\Omega_m$, and $\phi = 0$. The wavelength of the control field is 532 nm, and the power of the probe field is a hundred times less than the power of the corresponding control field.

where $M_1(\Omega) = \sqrt{\eta\kappa}C_1(\Omega)\Phi_p(\Omega)D_4(\Omega) + s_{mp}\theta_1(\Omega) + s_{mp}\theta_2(\Omega)$ and $M_2(\Omega) = C_2(\Omega)\{[(\Omega + i\tau)\Phi_p(\Omega) - 1]/Ga_0\}^2$ with $s_{mp} = s_m/s_p$, $s_p \neq 0$, and $s_m \neq 0$. The coherent mechanical driving leads to an additional second-order sideband with the amplitude $-\sqrt{\eta\kappa}[s_m\theta_1(\Omega) + s_m\theta_2(\Omega) + s_m^2 C_4(\Omega)e^{-2i\phi_m}]$ except for the second-order sideband induced by the probe field; thus one should expect an enhancement of the second-order sideband generation when the coherent mechanical pump is imposed on the optomechanical system.

The efficiency of second-order sideband generation η_s as a function of the frequency of the coherent mechanical pump Ω is shown in Fig. 1. The only difference between Panels (a)–(d) is the power of the control field. If the control field is lower than the threshold value, there is no optomechanically induced transparency signal [19–21]. In Fig. 1(a), we use a weak control field whose power is 10 μW to ensure that the effect of optomechanically induced transparency is absent: the probe field is almost completely absorbed near the resonance condition $\Omega = \omega_m$. First, we consider the case that the second-order sideband generation is totally induced by the probe field, viz., without the coherent mechanical pump. The efficiency of second-order sideband generation η_s is very small (the red solid line). The maximum value of η_s is about 0.75% which can be achieved at the resonance condition $\Omega = \omega_m$. As expected, the second-order sideband generation is enhanced when a coherent mechanical pump is imposed on the optomechanical system (shown by the dotted lines), and η_s increases as the amplitude of the mechanical pump increases. The maximum values of η_s are about 3.28, 7.34, and 19.94% corresponding to the amplitude of the mechanical pump at 0.5, 1, and 2 nN, respectively. We note that the condition of achieving the maximum value of η_s is not exactly the resonance condition $\Omega = \omega_m$ but shift a small frequency in the presence

of the mechanical pump. For $s_m = 2$ nN, the shift frequency is about $2 \times 10^{-4}\omega_m$.

For a stronger control field (the power of the control field is larger than the threshold value), the effect of optomechanically induced transparency occurs and a dip of the efficiency η_s arises at the resonance condition $\Omega = \omega_m$ in the absent of the coherent mechanical pump. In Fig. 1(b), the control field is 100 μW, and it is shown that η_s induced by the probe field reaches its local minimum at $\Omega = \omega_m$ (the red solid line). The two maximum values of η_s (about 2.77%), which are much larger than the weak control field case in Fig. 1(a), can be achieved symmetrically near the resonance condition $\Omega = \omega_m$. As shown by the dotted lines in Fig. 1(b), the second-order sideband generation is also enhanced by the coherent mechanical pump: the maximum value of η_s increases with the amplitude of the mechanical pump. However, the maximum value of η_s is about 9.55% corresponding to the 2 nN amplitude of the mechanical pump, which is much lower than the weak control field case in Fig. 1(a). We also note that the coherent mechanical driving induced enhancement of second-order sideband generation is mainly concentrated on the left side of the resonance condition $\Omega = \omega_m$. The enhancement is not obvious on the right side.

The dip deepens as the power of the control field increases. Without the mechanical pump, the maximum value of η_s is about 3.81 and 4.34% corresponding to the control field with powers 300 [Fig. 1(c)] and 600 μW [Fig. 1(d)]. In the presence of the mechanical pump, the second-order sideband generation is enhanced on the left side of the resonance condition $\Omega = \omega_m$ while subdued on the right side. The maximum values of η_s are about 6.41 [Fig. 1(c)] and 5.71% [Fig. 1(d)] corresponding to the 2 nN mechanical pump.

We can summarize the following features of coherent mechanical driving induced enhancement of second-order sideband generation from Fig. 1:

(i) The enhancement of second-order sideband generation is remarkable when the power of the control field is small, and η_s increases as the amplitude of the mechanical pump increases.

(ii) As the power of the control field increases, the second-order sideband generation is subdued instead of being enhanced as expected in the presence of a coherent mechanical pump. Under the same 2 nN mechanical pump, the maximum value of η_s decreases with the power of the control field. It should be stressed that the conclusions are obtained by fixing the phase difference.

(iii) Increasing the amplitude of the mechanical pump does not always bring an enhancement of second-order sideband generation. Second-order sideband generation is subdued on the right side of the resonance condition $\Omega = \omega_m$ when the control field is strong enough.

IV. PHASE-DEPENDENT EFFECTS OF SECOND-ORDER SIDEBAND GENERATION

The analytical expression of the efficiency of second-order sideband generation, viz., Eq. (13), shows that the second-order sideband generation is phase dependent. In what follows we will show that the phase difference ϕ between ϕ_m and ϕ_p plays an important role in the process of second-order sideband generation.

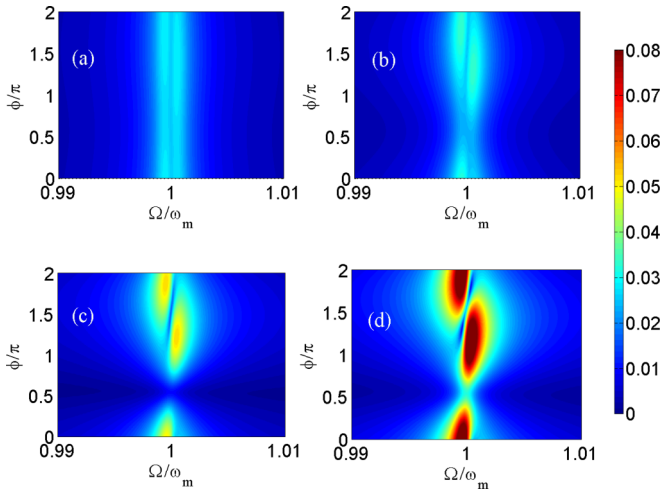

FIG. 2. (Color online) The efficiency of second-order sideband generation η_s varies with Ω and ϕ under different external mechanical pumps. $s_m =$ (a) 0.05, (b) 0.3, (c) 1.0, and (d) 2.0 nN. We use $\Omega_m/2\pi = 51.8$ MHz, $m = 20$ ng, $G/2\pi = -12$ GHz/nm, $\Gamma_m/2\pi = 41.0$ kHz, $\kappa/2\pi = 15.0$ MHz, and $\Delta = -\Omega_m$. The wavelength of the control field is 532 nm, and the powers of the control and probe fields are 0.1 mW and 1 μW, respectively.

Figure 2 shows η_s varies with Ω and ϕ under different external mechanical pumps. In Fig. 2(a), the external mechanical pump is weak and the second-order sideband generation is mainly induced by the probe field. The two bright lines correspond to the two maximum values of η_s, while the dark line corresponds to the dip at the the resonance condition $\Omega = \omega_m$. There is hardly any phase-dependent effects shown in Fig. 2(a), and the efficiency of second-order sideband generation is low (the colors are mainly blue or pale blue). As the amplitude of the external mechanical pump increases, the maximum value of η_s is enhanced. From Fig. 2(b) to Fig. 2(d), the amplitudes of the mechanical pump are 0.3, 1.0, and 2.0 nN, respectively. The emergence of the yellow zone in Fig. 2(c) and the red zone in Fig. 2(d) confirms the enhancement of the efficiency of second-order sideband generation. The parameter range of getting robust second-order sideband generation becomes wider and wider as the mechanical pump goes up.

Another typical feature of the second-order sideband generation with a coherent mechanical pump is the phase-dependent effect, which is absent if the mechanical pump is weak or absent. With the strengthening of the mechanical pump, the phase-dependent effect beginning to appear [Fig. 2(b)], and becomes remarkable when the mechanical pump is strong [Figs. 2(c) and 2(d)]. The phase-dependent effect occurs near the resonance condition $\Omega = \omega_m$. The parameter range of getting a robust phase-dependent effect also becomes wider and wider as the amplitude of the mechanical pump goes up. Such a phase-dependent effect makes the second-order sideband generation more tunable in the coherent-mechanical pumped optomechanical system, and the process of the second-order sideband generation can be tuned flexibly by the combination of the control and probe fields, and the mechanical pump.

V. CONCLUSION

In conclusion, we have discussed the second-order sideband generation in a coherent-mechanical pumped optomechanical system. The analytical expressions that describe the amplitude of the first- and second-order sideband are obtained. We found that the features of the coherent mechanical driving induced enhancement of second-order sideband generation are radically distinct between the weak control field case and the strong control field case. In the weak control field case, the effect of optomechanically induced transparency is absent and the efficiency of second-order sideband generation increases as the amplitude of the mechanical pump increases. In the strong control field case, the effect of optomechanically induced transparency occurs and the second-order sideband generation is subdued. In this case, increasing the amplitude of the mechanical pump does not always bring an enhancement of second-order sideband generation. Furthermore, we discussed the phase-dependent effect of the second-order sideband generation with a coherent mechanical pump, and showed that the phase difference ϕ plays an important role in the process of second-order sideband generation.

[1] M. Aspelmeyer, T. J. Kippenberg, and F. Marquardt, Rev. Mod. Phys. **86**, 1391 (2014).
[2] P. Meystre, Ann. Phys. (N.Y.) **525**, 215 (2013).
[3] H. Xiong, L. Si, X. Lü, X. Yang, and Y. Wu, Sci. China Phys. Mech. Astron. **58**, 050302 (2015).
[4] H. Xiong, L.-G. Si, A.-S. Zheng, X. Yang, and Y. Wu, Phys. Rev. A **86**, 013815 (2012).
[5] F. Marino and F. Marin, Phys. Rev. E **87**, 052906 (2013).
[6] P. Rabl, Phys. Rev. Lett. **107**, 063601 (2011).
[7] W. Z. Jia, L. F. Wei, Y. Li, and Y.-x. Liu, Phys. Rev. A **91**, 043843 (2015).
[8] X.-W. Xu and Y. Li, arXiv:1504.08069 [quant-ph].
[9] K. Børkje, A. Nunnenkamp, J. D. Teufel, and S. M. Girvin, Phys. Rev. Lett. **111**, 053603 (2013).
[10] A. Kronwald and F. Marquardt, Phys. Rev. Lett. **111**, 133601 (2013).
[11] M.-A. Lemonde, N. Didier, and A. A. Clerk, Phys. Rev. Lett. **111**, 053602 (2013).
[12] Y. C. Liu, Y. F. Xiao, Y. L. Chen, X. C. Yu, and Q. Gong, Phys. Rev. Lett. **111**, 083601 (2013).
[13] Y. Li and K. Zhu, Photon. Res. **1**, 16 (2013).
[14] A. D. O'Connell *et al.*, Nature (London) **464**, 697 (2010).
[15] J. Bochmann, A. Vainsencher, D. D. Awschalom, and A. N. Cleland, Nat. Phys. **9**, 712 (2013).
[16] L. Fan, K. Y. Fong, M. Poot, and H. X. Tang, Nat. Commun. **6**, 5850 (2015).
[17] T. Carmon, H. Rokhsari, L. Yang, T. J. Kippenberg, and K. J. Vahala, Phys. Rev. Lett. **94**, 223902 (2005).
[18] M. O. Scully, S. Y. Zhu, and A. Gavrielides, Phys. Rev. Lett. **62**, 2813 (1989).
[19] S. Weis *et al.*, Science **330**, 1520 (2010).
[20] A. H. Safavi-Naeini *et al.*, Nature (London) **472**, 69 (2011).
[21] J. B. Khurgin, M. W. Pruessner, T. H. Stievater, and W. S. Rabinovich, Phys. Rev. Lett. **108**, 223904 (2012).